Asymmetry of Peripapillary Retinal Blood Vessel and Retinal Nerve Fiber Layer Thickness Between Healthy Right and Left Eyes

Jack Quach,[1,2] Glen P. Sharpe,[1] Shaban Demirel,[3] Christopher A. Girkin,[4] Christian Y. Mardin,[5] Alexander F. Scheuerle,[6] Claude F. Burgoyne,[3] Balwantray C. Chauhan,[1] and Jayme R. Vianna[1]

[1]Department of Ophthalmology and Visual Sciences, Dalhousie University, Halifax, Nova Scotia, Canada
[2]Faculty of Health, Dalhousie University, Halifax, Nova Scotia, Canada
[3]Devers Eye Institute, Portland, Oregon, United States
[4]Department of Ophthalmology, University of Alabama at Birmingham, Alabama, United States
[5]Department of Ophthalmology, University of Erlangen, Erlangen, Germany
[6]Department of Ophthalmology, University of Heidelberg, Heidelberg, Germany

Correspondence: Jayme R. Vianna, Dalhousie University Department of Ophthalmology and Visual Sciences, 1276 South Park Street, Victoria Building, Room 2035, Halifax, Nova Scotia B3H 2Y9, Canada; jayme.vianna@dal.ca.

Received: May 16, 2022
Accepted: January 19, 2023
Published: February 15, 2023

Citation: Quach J, Sharpe GP, Demirel S, et al. Asymmetry of peripapillary retinal blood vessel and retinal nerve fiber layer thickness between healthy right and left eyes. *Invest Ophthalmol Vis Sci.* 2023;64(2):17. https://doi.org/10.1167/iovs.64.2.17

Purpose. The purpose of this study was to determine if there is asymmetry in retinal blood vessel (RBV) position and thickness between right and left eyes (R-L) and evaluate whether R-L asymmetry in RBV thickness is related to R-L asymmetry of retinal nerve fiber layer thickness (RNFLT).

Methods. We analyzed peripapillary circle scan optical coherence tomography (OCT) examinations from healthy White subjects to measure RNFLT and RBV thickness and position relative to the fovea to Bruch's membrane opening axis, for all visible RBV. The R-L asymmetries of RNFLT and RBV thickness were computed for each A-scan. Four major vessels (superior temporal artery [STA] and superior temporal vein [STV], inferior temporal artery [ITA], and vein [ITV]) were identified using infrared images.

Results. We included 219 individuals. The mean (standard deviation) number of RBV measured per eye was 15.0 (SD = 2.2). The position of the STV and STA was more superior in left eyes than in right eyes, by 2.4 degrees and 3.7 degrees, respectively ($P < 0.01$). There was no region with significant R-L asymmetry in RBV thickness. RNFLT was thicker in right eyes in the temporal superior region and thicker in left eyes in the superior and nasal superior regions, with the asymmetry profile resembling in a "W" shape. This shape was also present in post hoc analyses in two different populations. The R-L asymmetries of RBV and RNFLT at each A-scan were not significantly associated ($P = 0.37$).

Conclusions. There is little R-L asymmetry in RBV, and it is not related to RNFLT asymmetry. This study suggests that R-L RNFLT asymmetry is due to factors other than RBV.

Keywords: retinal nerve fiber layer (RNFL), retinal blood vessels (RBVs), asymmetry

Measurements of peripapillary retinal nerve fiber layer thickness (RNFLT) with optical coherence tomography (OCT) are routinely used for the diagnosis and follow-up of glaucoma.[1] However, there is large interindividual and interocular variability in RNFLT, which makes detecting early pathological changes challenging. For example, in an individual with moderately lower RNFLT in an eye, that eye could either have early pathological RFNLT loss or a physiologically normal RNFLT. A better understanding of factors related to RNFLT variability could allow us to derive more precise normative values and enhance the diagnostic accuracy of RNFLT measurements.

Previous research shows varying results regarding peripapillary RNFLT asymmetry between healthy right and left eyes.[2–14] Global averages in RNFLT are similar between right and left eyes,[4–7,12,13,15] but several studies have reported significant sectoral differences. The superior quadrant RNFLT is usually thicker in left eyes[4–7,9,11–13,16] whereas the nasal, temporal, and inferior quadrants of the RNFLT are usually thicker in right eyes.[2–7,9,11,12]

Although these reports have contributed to the characterization of normal right-to-left asymmetry (R-L) in RNFLT, none of them explored possible causes for these observed asymmetries. Furthermore, they focused on sectoral RNFLT asymmetries, potentially overlooking variations within each sector.

A potential factor determining R-L asymmetry in RNFLT could be the position of retinal blood vessels (RBVs). RNFLT is greater near RBV,[17–23] and the variability in the position and thickness of RBV contributes to the interindivid-

Copyright 2023 The Authors

This work is licensed under a Creative Commons Attribution-NonCommercial-NoDerivatives 4.0 International License.

ual variability in RNFLT measurements.[16–23] The association between RBV and RNFLT occurs in part because the RBV are included within the OCT-measured RNFLT, however, other factors could also be contributory.[17,21] For example, in addition to retinal ganglion cell axons, the RNFL also contains glial tissue,[24] which may be concentrated around RBV.[25] In addition, RNFL axonal distribution may influence the development of RBVs[26–28] as retinal neurons promote RBV development by providing trophic support.[29]

The purpose of our study was to assess whether there is an R-L asymmetry in the position and thickness of RBV and whether RBV thickness asymmetry relate to R-L asymmetry of RNFLT in healthy subjects. We aimed to precisely characterize the RBV and RNFLT asymmetry by evaluating their continuous profile around the peripapillary retina, measured relative to the fovea to Bruch's membrane opening (FoBMO) axis. We hypothesized that R-L asymmetries of RBV and RNFLT are associated, and that a greater understanding of this relationship could reveal sources of RNFLT variability.

Methods

Participants

We used data from a previous cross-sectional multicenter (5 centers; Dalhousie University, Denvers Eye Institute, University of Alabama at Birmingham, University of Erlangen, and University of Heidelberg) study which included healthy participants of self-reported European descent.[23] To be included in the study, participants met the criteria of: (1) age between 18 and 90 years, (2) clinically normal eye examination results, (3) intraocular pressure of 21 mm Hg or less, (4) best-corrected visual acuity of 20/40 or better, (5) refractive error within 6 diopters spherical equivalent and 2D astigmatism, and (6) normal visual field (Humphrey Field Analyzer; Carl Zeiss Meditec, Dublin, CA, USA, program 24-2 SITA) with normal glaucoma hemifield test and mean deviation within normal limits. Participants were excluded if the following were found: (1) unreliable visual field examination results based on the reliability indices and the perimetrist's notes, (2) optic nerve head photographs of insufficient quality, (3) OCT images of insufficient quality (image quality score <20 or presence of artifacts), or (4) missing data from one or both eyes. The study was approved by the Ethics Review Board at each of the institutions. In accordance with the Declaration of Helsinki, participants gave written informed consent to participate.

Optical Coherence Tomography

Participants were imaged with the Spectralis OCT (Heidelberg Engineering, Heidelberg, Germany). To position the scans, the operator used live B-scans to identify the foveal pit and four Bruch's membrane opening (BMO) points. Based on these points, the device software estimated the center of BMO and FoBMO axis, which served as reference framework for the scans. We used the 3.5 mm diameter circular peripapillary scan. Each image represented the average of 100 B-scans and each B-scan comprised of 768 A-scans (Figs. 1, 2). The device software automatically segmented and measured the RNFLT. The segmentation was manually checked and corrected if necessary. When performing the OCT scans, axial length and corneal curvature were entered into the device software to provide accurate scaling of measurements. Values of RNFLT for each A-scan were exported for analysis.

RBV Measurements

Using the OCT system software (Heidelberg Eye Explorer, Heidelberg Engineering), we manually identified the edges of all measurable RBVs located within the RNFL (see Fig. 2) and recorded the A-scan where each edge was positioned (768 possible positions, corresponding to each A-scan in the B-scan). The thickness of each RBV was measured in pixels corresponding to the number of A-scans between the RBV edges (each pixel corresponding to 1 A-scan). Vessels narrower than 2 pixels could not be consistently identified and were not measured.

Assuming the RBV cross-sections visualized on the OCT images are approximately squares, the RBV thickness along the circle scan (i.e. horizontally in the OCT image) was used as a surrogate for the antero-posterior RBV thickness (i.e. vertically in the OCT image). However, on some occasions, an RBV could be sectioned diagonally on the OCT image, resulting in an overestimation of the RBV antero-posterior thickness. To account for this, we set a maximum RBV antero-posterior thickness value of 12 pixels. This maximum thickness value was chosen after reviewing images of the thicker RBV measured.

The total RBV thickness for each A-scan was computed as the sum of the antero-posterior thickness of all RBV present in that A-scan. The anatomic position of each A-scan was converted to angular value (each A-scan corresponding to 0.468 degrees) measured from the FoBMO axis and increasing clockwise on the right eyes and counterclockwise on the left eyes. Therefore, 0 degrees

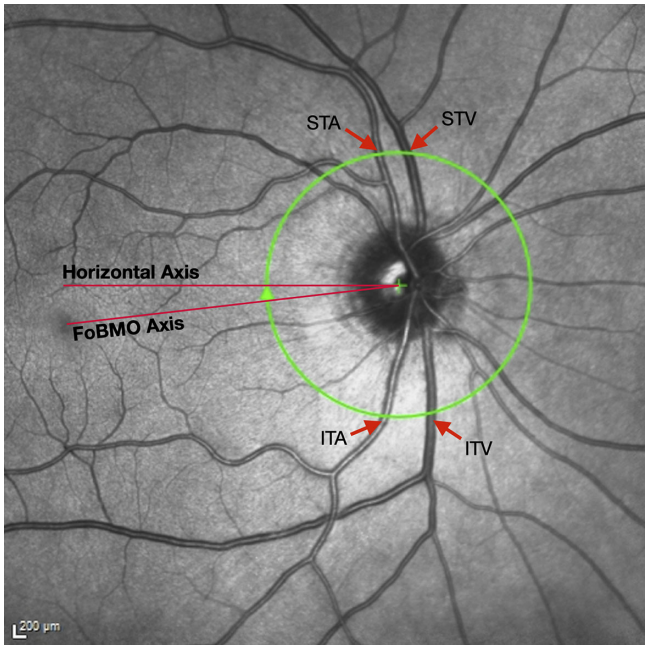

Figure 1. Example of infrared fundus image showing the position and size of the 3.5 mm circular scan pattern with optical coherence tomography. The fovea to Bruch's membrane opening (FoBMO) axis and the measured major retinal blood vessels is indicated in the image. STA, superior temporal artery; STV, superior temporal vein; ITA, inferior temporal artery; ITV, inferior temporal vein.

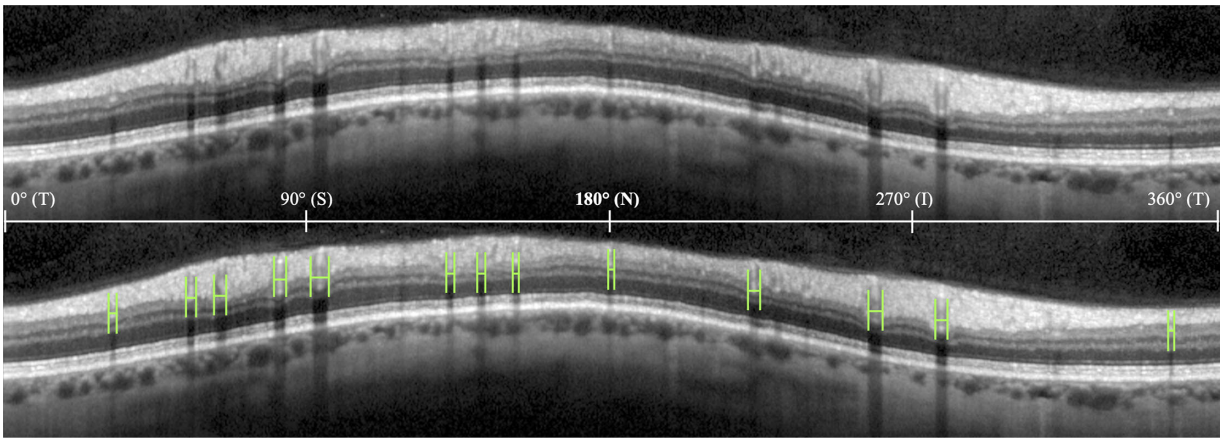

Figure 2. Example of retinal blood vessel (RBV) measurement, in the same eye presented in Figure 1. *Top*: Optical coherence tomography image of a peripapillary retinal nerve fiber layer scan. *Bottom*: Same image as the *top*, with overlays in *green* showing the RBV limits. The A-scan number of the two limit points were recorded by an investigator. Quadrants: T = temporal, S = superior, N = nasal, and I = inferior.

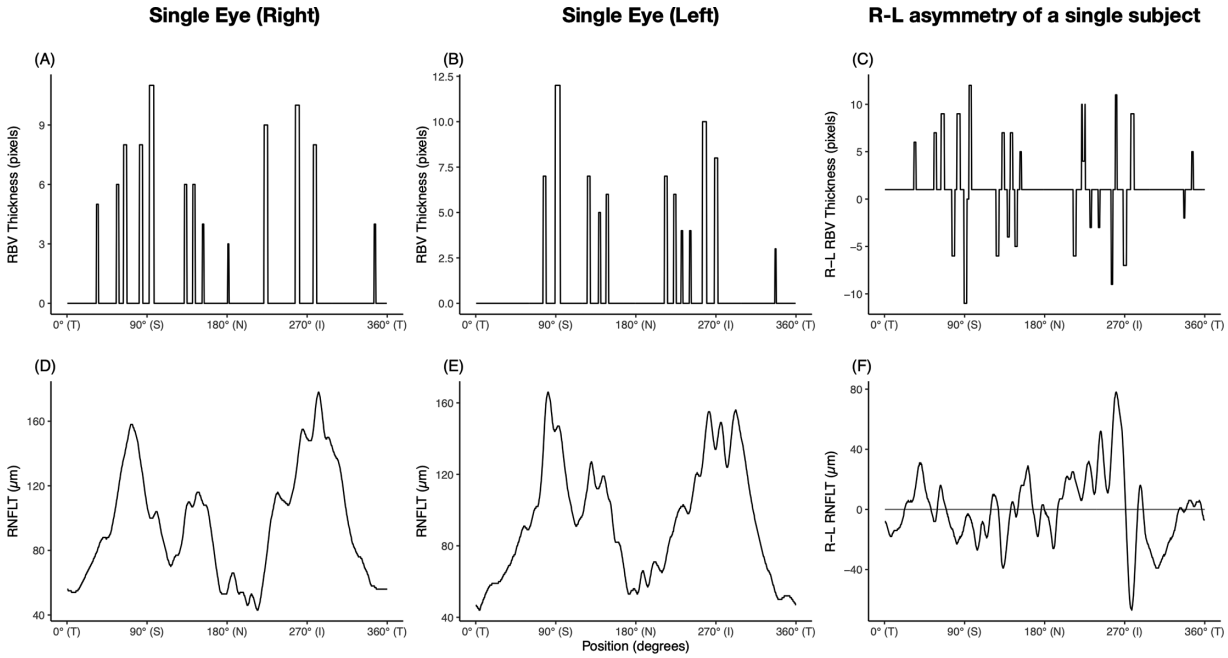

Figure 3. Examples of profiles of retinal blood vessel thickness (RBV, panels **A, B, C**, *top*) and retinal nerve fiber layer thickness (RNFLT, panels **D, E, F**, *bottom*) from a study participant, the same participant presented in Figures 1 and 2. **A** and **D** Profiles for the participant's right eye. **B** and **E** Profiles for the participant's left eye. **C** and **F** Profiles for the participant's right eye minus left eye asymmetry (R-L). T = temporal, S = superior, N = nasal, and I = inferior.

corresponds to the FoBMO axis (temporal region) and 90 degrees corresponds to the superior region, in all eyes.

Using the OCT infrared image, four major RBV per eye were classified as follows: superior temporal artery (STA), superior temporal vein (STV), inferior temporal vein (ITV), and inferior temporal artery (ITA; see Fig. 1). If these vessels had branched closer to the optic nerve than the OCT scan, the thickest branch was selected. The angular position of a major RBV was defined as being midway between the two vessel edges.

All RBV measurements were made by the same observer who has experience in OCT image segmentation. To estimate intra-observer reproducibility of the RBV position and thickness, measurements were repeated in a random subsample of five participants (10 eyes and 155 RBVs).

Data Analysis

Comparison of ocular characteristics and major RBV positions between right and left eyes were made using paired *t*-tests. The asymmetry between RNFLT and RBV thickness in right and left eyes of each participant were calculated for each A-scan by subtracting thickness values between the participant's right and left eyes (Fig. 3). Then, for each A-scan, the mean asymmetry of all participants was computed and plotted to visualize their profiles (Figs. 4, 5). To assess the association between mean R-L asymmetry of RBV

Investigative Ophthalmology & Visual Science

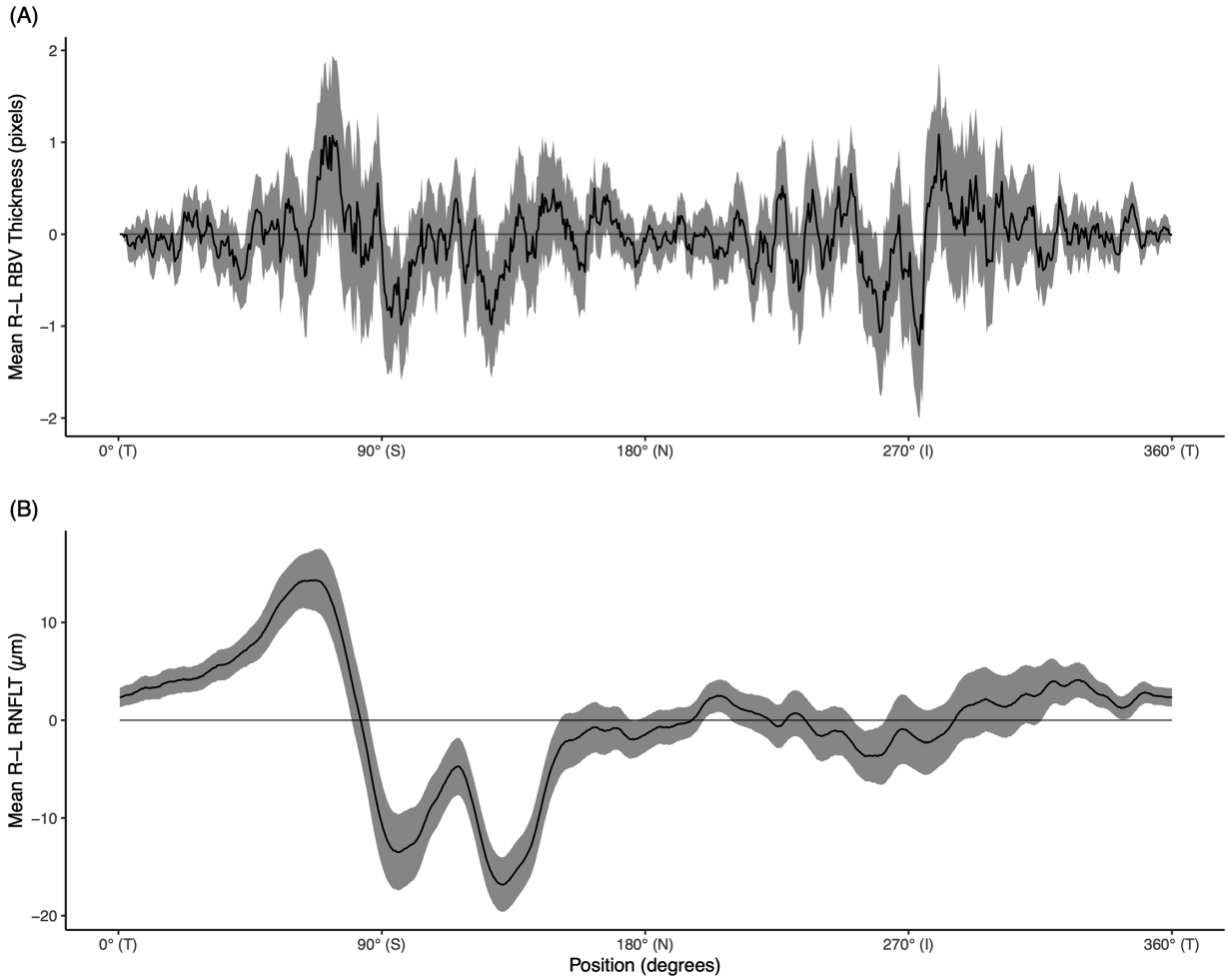

Figure 4. (**A**) Profile of mean right eye minus left eye (R-L) retinal nerve fiber layer thickness (RNFLT) asymmetry for all participants shown by the *black line*. (**B**) Profile of mean R-L retinal blood vessel (RBV) thickness asymmetry for all participants shown by the black line. The 95% confidence intervals of the mean are indicated by the shaded area. T = temporal, S = superior, N = nasal, and I = inferior.

thickness and mean R-L asymmetry of RNFLT, we used a generalized least squares model,[30] because it was necessary to account for the correlation between observations (i.e. the data from each A-scan is not independent, as A-scans close to each other tend to be similar). Values were reported as mean (standard deviation), unless stated otherwise. The P values < 0.05 were considered statistically significant. Analyses were performed using R open-source statistical programming software (available at www.r-project.org, version 3.6.0), including package "nlme" (version 3.1.139).

Post Hoc Analysis

To evaluate the reproducibility and generalizability of our findings, we performed a post hoc analysis of the profile of mean R-L RNFLT asymmetry in a Brazilian and Japanese population using data from previous normative OCT studies with similar data collection.[31,32]

Results

We included both eyes each of 219 participants who had a mean age of 50.9 years (17.8; range = 19.9–87.9 years). The mean number of RBV measured per eye was 14.9 (2.2). Two hundred one (201) vessels had a thickness value of greater than 12 pixels, out of 6556 vessels measured. The mean RBV thickness was 6.2 (2.9) pixels. Table 1 reports characteristics of the studied right and left eyes. The axial length was greater in left eyes than in right eyes by 0.05 mm ($P = 0.02$), and the BMO area was greater in right eyes than in left eyes by 0.05 mm^2 ($P < 0.01$). Global RNFLT was not statistically different between right and left eyes ($P = 0.91$).

In the subsample of participants who were measured twice, the RBV position reproducibility was high, with mean difference between 2 measurements of 0.2 degrees (0.2). The RBV thickness reproducibility was also high, with a mean difference between the 2 measurements of 0.8 (0.7) pixels.

The comparison of major RBV position asymmetry comparison is shown in Table 2. The STA and STV were statistically significantly more superior in the left eyes than in the right eyes, by 2.4 degrees (3.8) in the STA ($P = 0.01$) and by 3.6 degrees (15.8) in the STV ($P < 0.01$). The ITA and ITV position were not statistically significantly different between the right and left eyes.

The profile of mean R-L asymmetry of RBV thickness (see Fig. 4A) did not reveal a clear pattern; the magnitude was small and confidence intervals crossed in approximately all

Investigative Ophthalmology & Visual Science

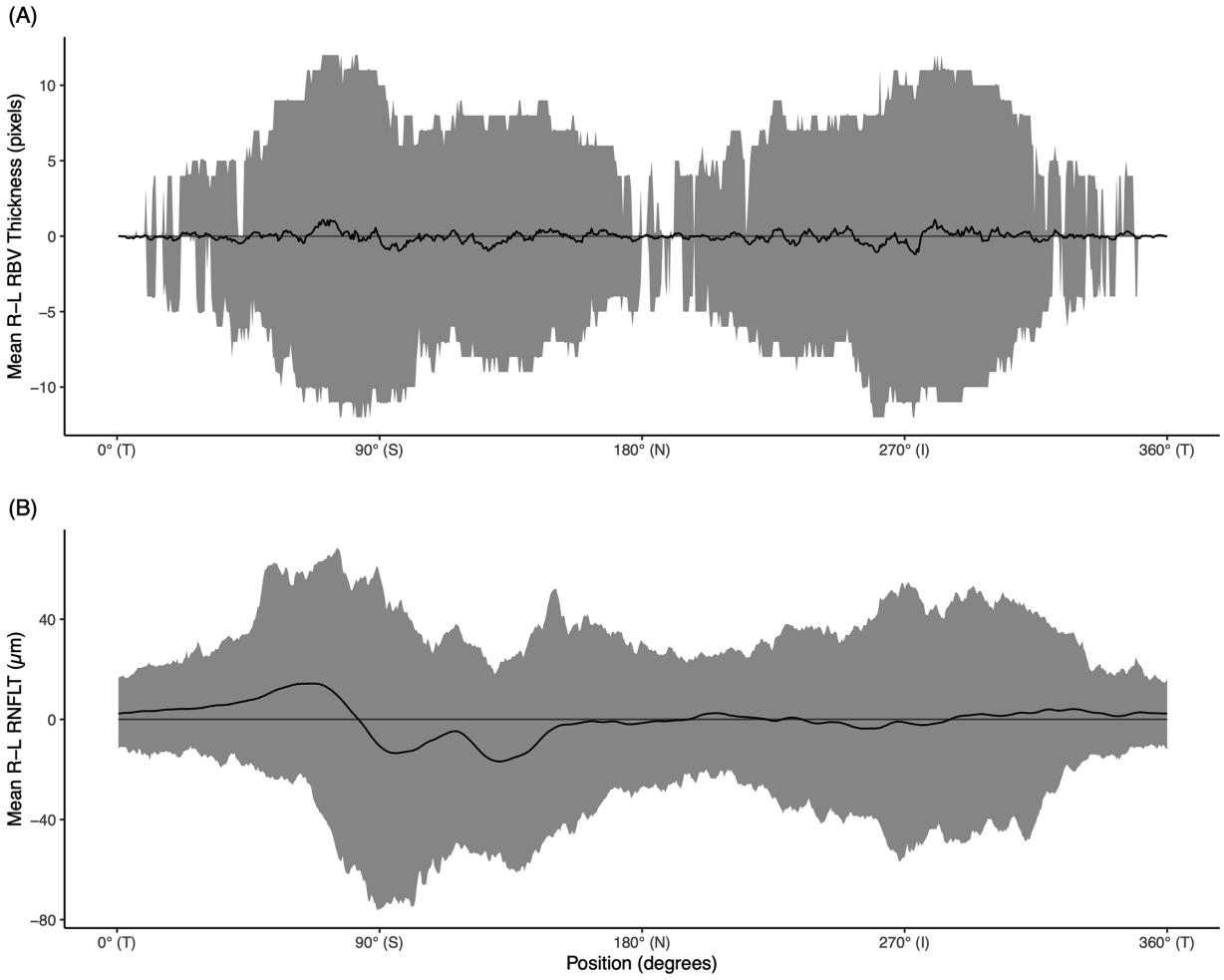

Figure 5. (**A**) Profile of mean right eye minus left eye (R-L) retinal nerve fiber layer thickness (RNFLT) asymmetry for all participants shown by the black line. (**B**) Profile of mean R-L retinal blood vessel (RBV) thickness asymmetry for all participants shown by the *black line*. The 95% distribution range (i.e. from percentile 2.5% to 97.5%) is indicated by the shaded area. T = temporal, S = superior, N = nasal, and I = inferior.

Table 1. Characteristics of Studied Eyes

Characteristic	Right Eye Value	Left Eye Value	Right-Left Asymmetry	*P* Value
Spherical equivalent (D)	−0.20 ± 1.67	−0.17 ± 1.78	−0.03 ± 0.75	0.67
Axial length (mm)	23.71 ± 0.92	23.66 ± 0.95	0.05 ± 0.28	0.02
BMO area (mm^2)	1.76 ± 0.37	1.81 ± 0.40	−0.05 ± 0.20	<0.01
Global RNFLT (μm)	97.19 ± 10.31	97.31 ± 10.10	−0.11 ± 3.62	0.91

Values are mean ± standard deviation. *P* value for paired *t*-test.
Abbreviations: BMO, Bruch's membrane opening; RNFLT, retinal nerve fiber layer thickness.

locations (see Fig. 4A). Right eyes had greater RNFLT in the superior temporal region, peaking at a mean of 14.3 μm at 62.8 degrees (see Fig. 4B). Left eyes had greater RNFLT in the superior and superior nasal region, with mean peaks at −13.6 μm at 95.2 degrees and −16.9 μm at 130.8 degrees, resembling a "W" shape (see Fig. 4B). Other positions had less remarkable R-L asymmetry of RNFLT. The 95% distribution range (i.e. from percentile 2.5% to 97.5%) of profiles

Table 2. Position of Major Retinal Blood Vessels in Right and Left Eyes

Retinal Blood Vessel	Right Eye Position (Degrees)	Left Eye Position (Degrees)	Right-Left Asymmetry (Degrees)	*P* Value
STA	74.82 ± 11.49	77.22 ± 12.84	−2.39 ± 13.84	0.01
STV	77.00 ± 12.48	80.65 ± 13.77	−3.66 ± 15.83	<0.01
ITA	286.14 ± 13.36	284.42 ± 13.95	1.72 ± 16.64	0.13
ITV	281.97 ± 15.03	280.88 ± 15.03	1.09 ± 19.12	0.41

Values are mean ± standard deviation. *P* value for paired *t*-test.
Abbreviations: ITA, inferior temporal artery; ITV, inferior temporal vein; STA, superior temporal artery; STV, superior temporal vein.

Investigative Ophthalmology & Visual Science

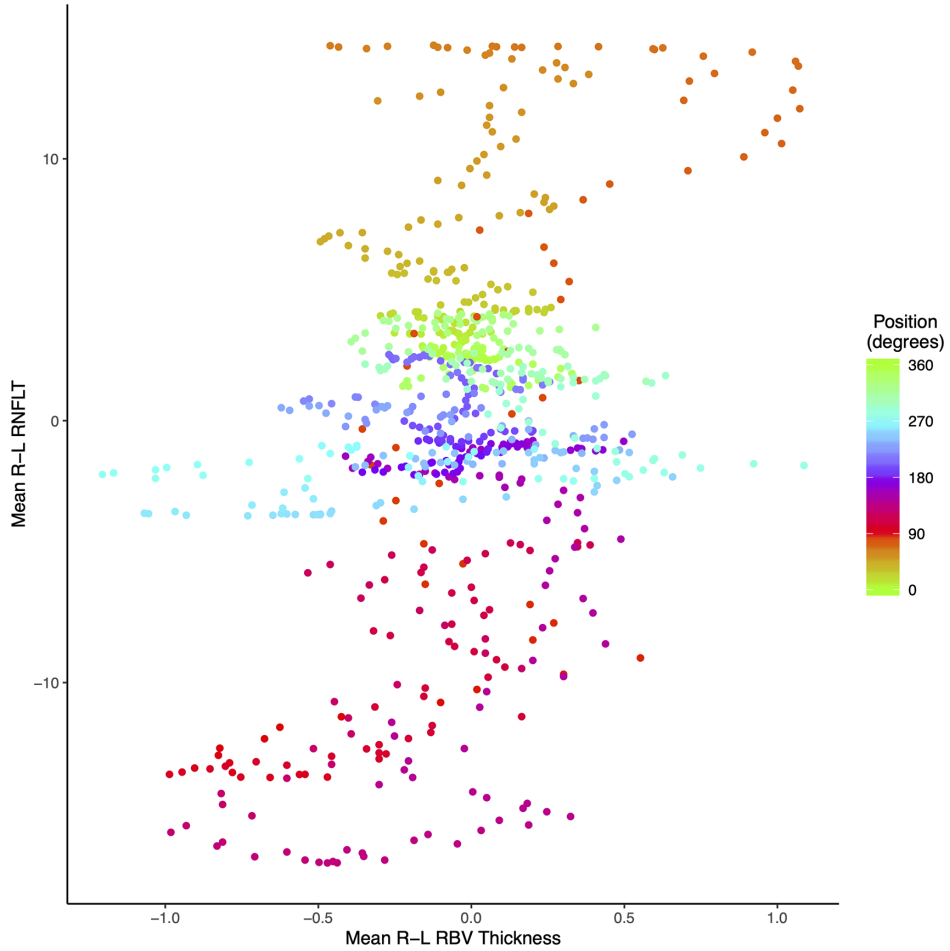

Figure 6. Scatterplot of mean right eye minus left eye (R-L) retinal blood vessel (RBV) thickness and mean R-L retinal nerve fiber layer thickness (RNFLT) in each A-scan. Points are color-graded to their position around the optic disc. Generalized least squares model did not show a significant association (beta 0.02, $P = 0.37$).

of mean R-L asymmetry of RNFLT and RBV thickness shows that individuals vary greatly in the degree of asymmetry (see Fig. 5). The generalized least squares model showed that there was no significant association between mean asymmetry of RBV thickness and RNFLT (beta 0.02, $P = 0.37$; Fig. 6).

The post hoc analysis of R-L RNFLT asymmetry profiles in a Brazilian and a Japanese population revealed a similar "W" shape in the supero-superonasal region as in the White population (Fig. 7).

Discussion

Our findings suggest that there is no significant R-L asymmetry of RBV position and thickness profile measured with OCT in healthy eyes. Although we found a small positional difference in the STA and STV, there was no such difference in the ITA and ITV. In addition, the profile of R-L asymmetry of RBV thickness (see Fig. 4A) did not suggest a clear pattern of asymmetry. We are not aware of previous published studies evaluating R-L asymmetry of RBV in a manner reported in this study, however, studies using other methodologies also did not find large asymmetries. Leung and colleagues[33] showed that the mean diameter of retinal arterial branches of right eyes was 3 µm larger than those of left eyes using a computer-assisted measurement of fundus photographs and a specific formula to compute standardized mean diameters. They found no differences in venular branches.[33] Using OCT angiography, Hou and colleagues[34] found that the inter-eye asymmetry of circumpapillary vessel density in healthy eyes was, on average, 1.7%, but they did not report R-L vessel width differences. It is also not clear whether OCT angiography is a suitable method to measure vessel width.

Similar to previous research,[4–7,9,11–13,16] we found that the RNFLT in the superior region is thicker in left eyes compared with right eyes, and in the temporal region is thicker in right eyes compared to left eyes. Some previous research reported the nasal and inferior regions to be thicker in right eyes,[2–7,9,11,12] although this was not found in our data. The use of different OCT devices and measurement methodologies may be related to the variability in findings among studies of interocular asymmetry.

In contrast to studies which performed analysis in sectors, we evaluated the R-L asymmetry in each A-scan and reported a more granular continuous asymmetry profile around the peripapillary retina (see Fig. 4B). This R-L RNFLT asymmetry profile has a "W" shape with a peak indicating larger right eye RNFLT in the temporal superior region and two troughs indicating larger left eye RNFLT in the superior and superior nasal regions. Because the 95% confidence interval

Investigative Ophthalmology & Visual Science

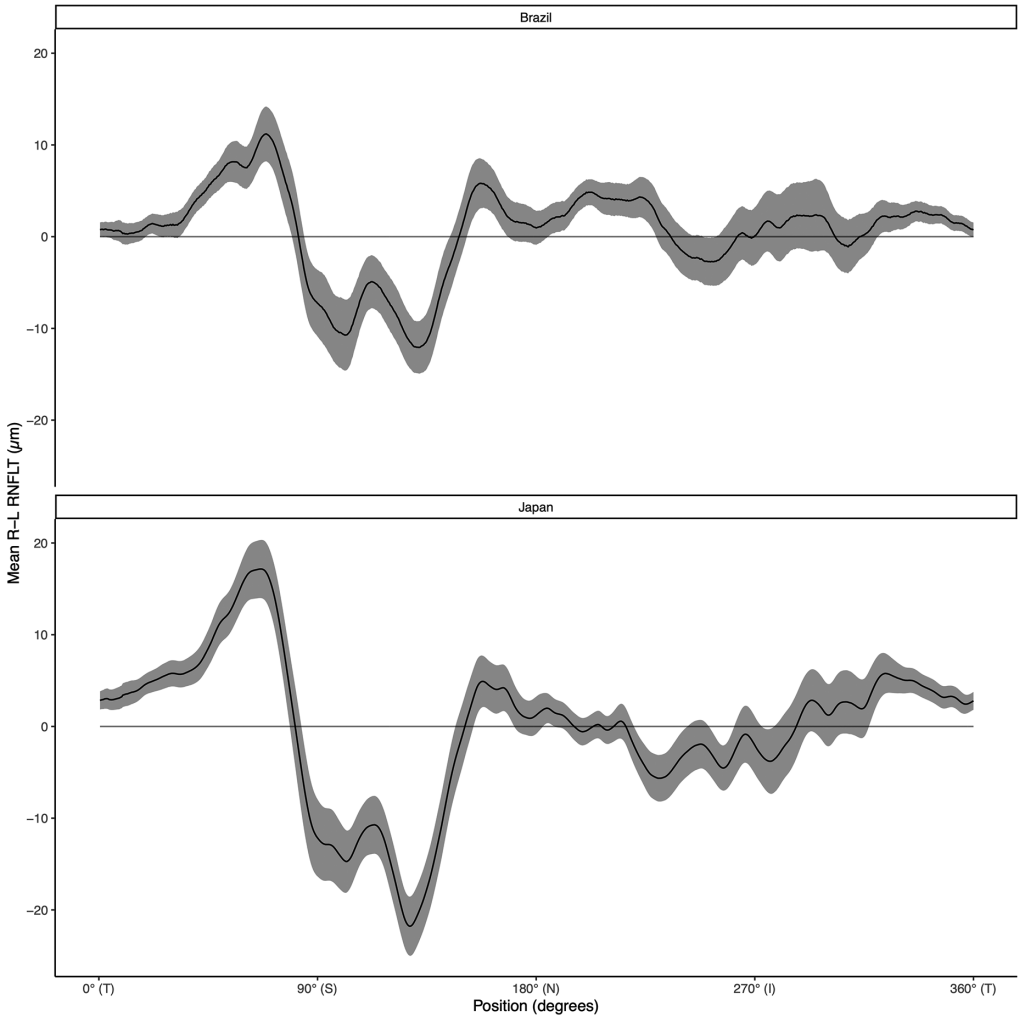

Figure 7. Profile of mean right eye minus left eye (R-L) retinal nerve fiber layer thickness (RNFLT) asymmetry for Brazilian (n = 220) and Japanese (n = 218) subjects shown by the *black lines*. The 95% confidence intervals of the mean are indicated by the shaded area. T = temporal, S = superior, N = nasal, and I = inferior.

of the mean in these regions consistently excluded zero (see Fig. 4B), this "W" pattern was statistically significant. In addition, the post hoc analysis in a Brazilian and Japanese population from previous normative OCT studies[31,32] revealed a similar "W" pattern (see Fig. 7). This consistent pattern across populations indicates a trend in R-L RNFLT asymmetry and may be a general feature of human eyes. Furthermore, two recently published studies reported profiles of R-L RNFLT asymmetry in large population samples from Germany.[35,36] Both studies found that right eyes had higher RNFLT values in the temporal superior region, whereas left eyes had higher values in the superior and nasal superior regions, similar to the pattern found in this study.

We hypothesized that RBV asymmetry would be significantly associated with RNFLT asymmetry, therefore suggesting that either one was due to the other, or that both were due to a similar causative factor. However, because we did not observe a clear pattern in the RBV asymmetry profile like the pattern observed in RNFLT asymmetry, nor did we observe a statistically significant association between RBV and RNFLT asymmetry, our findings do not support this hypothesis. Potential reasons that could cause the R-L RNFLT asymmetry are not clear, but numerous factors governing interocular symmetry in ocular and visual pathway development may underly RNFLT asymmetry and further studies are needed to explore them.[37]

Similarly, the FoBMO angle was significantly more negative in left eyes in previous studies[31,32] but there are still no clear explanations for this finding.

Whereas significant and reproducible, the observed pattern of R-L RNFLT asymmetry observed is primarily an indication of a populational trend; there is still large interindividual variability in R-L RNFLT asymmetry (see Fig. 5B). In other words, when averaging multiple individuals, the RNFLT will likely be thicker in the right or left eyes in regions according to the pattern we report. However, when observing an individual, it is common to observe R-L RNFLT asymmetry profiles that do not follow the pattern that is evident when looking at population average data. Clinicians should be careful when using asymmetries in RNFLT profiles in individual subjects to detect early glaucoma damage, but asymmetries larger than 30% to 40% could be considered suspicious.[14]

A strength of our study was the use of the FoBMO axis as a positioning reference for RBV and RNFLT measurements.

Investigative Ophthalmology & Visual Science

Many previous studies exploring R-L RNFLT asymmetry used a horizontal reference to position sectors,[2–9,11,12] which is not an anatomically consistent reference,[38] therefore making RNFLT measurements susceptible to influence of head tilt[39,40] and the magnitude of the FoBMO angle.[41] A limitation of our study was the assumption that RBV cross-sections were squares, therefore overestimating the vessel thickness near the edges of the vessels. However, because the mean RBV thickness asymmetries were small, this overestimation is unlikely to have influenced our results. Additionally, we do not have information regarding participants ocular dominance and non-ocular diseases therefore could not explore their effects in our findings.

In conclusion, there is no significant R-L asymmetry in RBV, and it is not related to RNFLT asymmetry. In contrast, a significant pattern of R-L asymmetry can be observed in RNFLT. To better understand R-L RNFLT asymmetry, other factors should be investigated.

Acknowledgments

The authors thank the investigators of the Brazilian normative study, Zangalli, Reis, Miguel-Neto, and Costa, as well as those of the Japanese normative study, Araie, Iwase, Sugiyama, Nakazawa, Tomita, Hangai, Yanagi, Murata, and Tanihara, for allowing us to use these studies' data.

Disclosure: **J. Quach**, None; **G.P. Sharpe**, None; **S. Demirel**, None; **C.A. Girkin**, National Eye Institute (F), Research to Prevent Blindness (F), EyeSight Foundation of Alabama (F), Heidelberg Engineering (research support) (F); **C.Y. Mardin**, None; **A.F. Scheuerle**, None; **C.F. Burgoyne**, National Institutes of Health R01 Awards (C), Heidelberg Engineering , instruments and unrestricted research support, no personal income or intellectual property (C); Life BioSciences (C); **B.C. Chauhan**, CenterVue (equipment support) (F), Heidelberg Engineering (research and equipment support) (F), Novartis (speaker bureau) (F), Topcon (equipment support) (F); **J.R. Vianna**, Eadietech (C)

References

1. Chen TC, Hoguet A, Junk AK, et al. Spectral-domain OCT: Helping the clinician diagnose glaucoma: A report by the American academy of ophthalmology. *Ophthalmology*. 2018;125(11):1817–1827.
2. Park JJ, Oh DR, Hong SP, Lee KW. Asymmetry analysis of the retinal nerve fiber layer thickness in normal eyes using optical coherence tomography. *Korean J Ophthalmol KJO*. 2005;19(4):281–287.
3. Huynh SC, Wang XY, Burlutsky G, Mitchell P. Symmetry of optical coherence tomography retinal measurements in young children. *Am J Ophthalmol*. 2007;143(3):518–520.
4. Budenz DL. Symmetry between the right and left eyes of the normal retinal nerve fiber layer measured with optical coherence tomography (an AOS thesis). *Trans Am Ophthalmol Soc*. 2008;106:252–275.
5. Qian J, Wang W, Zhang X, et al. Optical coherence tomography measurements of retinal nerve fiber layer thickness in Chinese children and teenagers. *J Glaucoma*. 2011;20(8):509–513.
6. Mwanza JC, Durbin MK, Budenz DL. Interocular symmetry in peripapillary retinal nerve fiber layer thickness measured with the cirrus HD-OCT in healthy eyes. *Am J Ophthalmol*. 2011;151(3):514–521.
7. Dalgliesh JD, Tariq YM, Burlutsky G, Mitchell P. Symmetry of retinal parameters measured by spectral-domain OCT in normal young adults. *J Glaucoma*. 2015;24(1):20–24.
8. Chen L, Huang J, Zou H, et al. Retinal nerve fiber layer thickness in normal Chinese students aged 6 to 17 years. *Invest Opthalmology Vis Sci*. 2013;54(13):7990.
9. Altemir I, Oros D, Elía N, Polo V, Larrosa JM, Pueyo V. Retinal asymmetry in children measured with optical coherence tomography. *Am J Ophthalmol*. 2013;156(6):1238–1243.
10. Jee D, Hong SW, Jung YH, Ahn MD. Interocular retinal nerve fiber layer thickness symmetry value in normal young adults. *J Glaucoma*. 2014;23(8):e125–e131.
11. Al-Haddad C, Antonios R, Tamim H, Noureddin B. Interocular symmetry in retinal and optic nerve parameters in children as measured by spectral domain optical coherence tomography. *Br J Ophthalmol*. 2014;98(4):502–506.
12. Hwang YH, Song M, Kim YY, Yeom DJ, Lee JH. Interocular symmetry of retinal nerve fibre layer thickness in healthy eyes: A spectral-domain optical coherence tomographic study. *Clin Exp Optom*. 2014;97(6):550–554.
13. Yang M, Wang W, Xu Q, Tan S, Wei S. Interocular symmetry of the peripapillary choroidal thickness and retinal nerve fibre layer thickness in healthy adults with isometropia. *BMC Ophthalmol*. 2016;16(1):182.
14. Zangalli CES, Reis ASC, Vianna JR, Vasconcellos JPC, Costa VP. Interocular asymmetry of minimum rim width and retinal nerve fiber layer thickness in healthy Brazilian individuals. *J Glaucoma*. 2018;27(12):1136–1141.
15. Park JJ, Oh DR, Hong SP, Lee KW. Asymmetry analysis of the retinal nerve fiber layer thickness in normal eyes using optical coherence tomography. *Korean J Ophthalmol*. 2005;19(4):281.
16. Ly A, Banh J, Luu P, Huang J, Yapp M, Zangerl B. Interocular asymmetry of the superonasal retinal nerve fibre layer thickness and blood vessel diameter in healthy subjects. *PLoS One*. 2019;14(12):e0226728.
17. Hood DC, Fortune B, Arthur SN, et al. Blood vessel contributions to retinal nerve fiber layer thickness profiles measured with optical coherence tomography. *J Glaucoma*. 2008;17(7):519–528.
18. Hood DC, Salant JA, Arthur SN, Ritch R, Liebmann JM. The location of the inferior and superior temporal blood vessels and interindividual variability of the retinal nerve fiber layer thickness. *J Glaucoma*. 2010;19(3):158–166.
19. Yamashita T, Asaoka R, Tanaka M, et al. Relationship between position of peak retinal nerve fiber layer thickness and retinal arteries on sectoral retinal nerve fiber layer thickness. *Invest Ophthalmol Vis Sci*. 2013;54(8):5481–5488.
20. Pereira I, Weber S, Holzer S, et al. Correlation between retinal vessel density profile and circumpapillary RNFL thickness measured with Fourier-domain optical coherence tomography. *Br J Ophthalmol*. 2014;98(4):538–543.
21. Patel NB, Sullivan-Mee M, Harwerth RS. The relationship between retinal nerve fiber layer thickness and optic nerve head neuroretinal rim tissue in glaucoma. *Invest Ophthalmol Vis Sci*. 2014;55(10):6802–6816.
22. Resch H, Pereira I, Weber S, Holzer S, Fischer G, Vass C. Retinal blood vessel distribution correlates with the peripapillary retinal nerve fiber layer thickness profile as measured with GDx VCC and ECC. *J Glaucoma*. 2015;24(5):389–395.
23. Chauhan BC, Danthurebandara VM, Sharpe GP, et al. Bruch's membrane opening minimum rim width and retinal nerve fiber layer thickness in a normal white population: A multicenter study. *Ophthalmology*. 2015;122(9):1786–1794.
24. Ogden TE. Nerve fiber layer of the primate retina: Thickness and glial content. *Vision Res*. 1983;23(6):581–587.
25. Vecino E, Rodriguez FD, Ruzafa N, Pereiro X, Sharma SC. Glia-neuron interactions in the mammalian retina. *Prog Retin Eye Res*. 2016;51:1–40.

26. Dorrell MI, Friedlander M. Mechanisms of endothelial cell guidance and vascular patterning in the developing mouse retina. *Prog Retin Eye Res*. 2006;25(3):277–295.
27. Carmeliet P, Tessier-Lavigne M. Common mechanisms of nerve and blood vessel wiring. *Nature*. 2005;436(7048):193–200.
28. Miller G. Developmental biology. Nerves tell arteries to make like a tree. *Science*. 2002;296(5576):2121–2123.
29. Famiglietti EV, Stopa EG, McGookin ED, Song P, LeBlanc V, Streeten BW. Immunocytochemical localization of vascular endothelial growth factor in neurons and glial cells of human retina. *Brain Res*. 2003;969(1-2):195–204.
30. Pinheiro J, Bates D. *Mixed-Effects Models in S and S-PLUS*. New York, NY: Springer; 2000.
31. Zangalli CS, Vianna JR, Reis ASC, et al. Bruch's membrane opening minimum rim width and retinal nerve fiber layer thickness in a Brazilian population of healthy subjects. *PLoS One*. 2018;13(12):e0206887.
32. Araie M, Iwase A, Sugiyama K, et al. Determinants and characteristics of Bruch's membrane opening and Bruch's membrane opening-minimum rim width in a normal Japanese population. *Invest Ophthalmol Vis Sci*. 2017;58(10):4106–4113.
33. Leung H, Wang JJ, Rochtchina E, et al. Computer-assisted retinal vessel measurement in an older population: Correlation between right and left eyes. *Clin Experiment Ophthalmol*. 2003;31(4):326–330.
34. Hou H, Moghimi S, Zangwill LM, et al. Inter-eye asymmetry of optical coherence tomography angiography vessel density in bilateral glaucoma, glaucoma suspect, and healthy eyes. *Am J Ophthalmol*. 2018;190:69–77.
35. Baniasadi N, Rauscher FG, Li D, et al. Norms of interocular circumpapillary retinal nerve fiber layer thickness differences at 768 retinal locations. *Transl Vis Sci Technol*. 2020;9(9):23.
36. Wagner FM, Hoffmann EM, Nickels S, et al. Peripapillary retinal nerve fiber layer profile in relation to refractive error and axial length: Results from the gutenberg health study. *Transl Vis Sci Technol*. 2020;9(9):35.
37. Cameron JR, Megaw RD, Tatham AJ, et al. Lateral thinking - Interocular symmetry and asymmetry in neurovascular patterning, in health and disease. *Prog Retin Eye Res*. 2017;59:131–157.
38. Chauhan BC, Burgoyne CF. From clinical examination of the optic disc to clinical assessment of the optic nerve head: A paradigm change. *Am J Ophthalmol*. 2013;156(2):218–227.e2.
39. Bin Ismail MA, Hui Li Lilian K, Yap SC, Yip LW. Effect of head tilt and ocular compensatory mechanisms on retinal nerve fiber layer measurements by cirrus spectral domain and spectralis optical coherence tomography in normal subjects. *J Glaucoma*. 2016;25(7):579–583.
40. Mohammad S, Jarrar FS, Torres LA, Sharpe GP, Vianna JR, Chauhan BC. Impact of head tilt on optical coherence tomography image orientation. *J Glaucoma*. 2018;27(12):1042–1045.
41. Jonas RA, Wang YX, Yang H, et al. Optic disc - fovea angle: The Beijing eye study 2011. *PLoS One*. 2015;10(11):e0141771.

Investigative Ophthalmology & Visual Science